NATIONAL ACADEMY OF SCIENCES

Number 22 • April 1959

IGY BULLETIN

A monthly survey by the U. S. National Committee for the International Geophysical Year. Established by and part of the National Academy of Sciences, the Committee is responsible for the U. S. International Geophysical Year program in which several hundred American scientists are participating and many public and private institutions are cooperating.

The Floor of the Arctic Ocean

This report is based on a paper given by Kenneth Hunkins, now of the Geophysics Department, Stanford University, at the IGY Symposium during the 125th Meeting of the American Association for the Advancement of Science, Washington, D. C., December 29–30, 1958.

Among the many IGY scientific programs carried out on Drifting Station Alpha, in the Arctic Ocean, were marine geophysics studies directed by the Lamont Geological Observatory of Columbia University and supported by the Terrestrial Sciences Branch of the Air Force Cambridge Research Center. The studies included seismology, gravimetry, earth magnetism, physical oceanography, and measurement of ice drift and currents.

The drifting station, on a ten-foot-thick ice floe, provided a relatively stable platform for this work, in contrast to the rolling and pitching of a research vessel. Moreover, the slow drift of the floe allowed time for detailed study of the ocean bottom, although the floe's irregular and uncertain course somewhat limited the area of coverage. Between June 8, 1957, when celestial navigation began, and November 1, 1958, when the station was evacuated because of break-up of the floe, the total drift, within an area roughly 300 mi square, was 1830 statute mi (see Fig. 1). The average drift was 3½ mi/day.

This report presents some results of investigations of the Arctic Ocean floor and the upper few feet of underlying sediment. The methods used in these studies were seismic echo soundings, dredge hauls of bottom material, submarine photography, and bottom coring and "grab" sampling.

Topography and Structure of the Bottom

Echo soundings provided data on the topography of the bottom. Once or twice a day a small dynamite charge was ex-

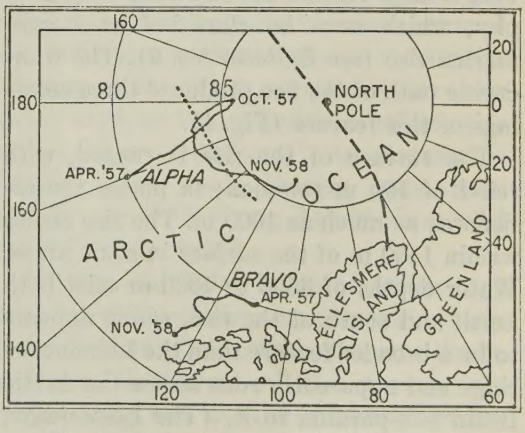

Fig. 1. *Movement of US-IGY Drifting Stations Throughout Most of the IGY Period. Dashed line represents approximate crest line of Lomonosov ridge; dotted line represents approximate crest of submarine rise discovered from Drifting Station Alpha.*

ploded and the reflections recorded by the seismograph. An array of 12 geophones on the ice served as detectors, allowing the attitude of the reflecting surface to be determined. These spot echo soundings were usually made 1–3 mi apart, depending on the rate of drift. The strike and dip of the bottom, as well as the depth, were measured with each shot. Dips of the ocean floor ranged from 0° to 28°. Although complete analysis of all data has not yet been made, it appears that dips of 2°-3° are most characteristic in this area. (See Fig. 2.)

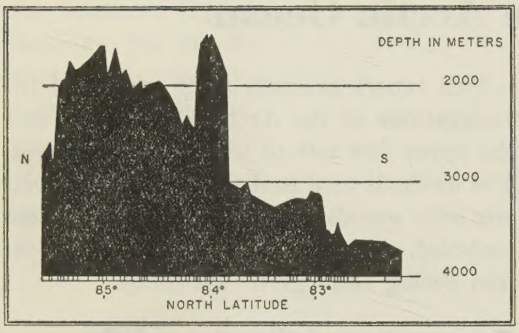

Fig. 2. *Profile of Arctic Ocean Floor Approximately Along the 167°W Meridian. Vertical exaggeration is 100:1.*

Submarine Ridge: Throughout most of the time the station was occupied, it drifted over a large feature of rough, high topography, which may be classified as a submarine rise (see *Bulletin No. 6*). The wandering path of the floe produced three crossings of this feature (Fig. 1).

The surface of the rise is rugged, with relief of 100 m common; in places the relief was as much as 1000 m. The rise comes within 1400 m of the surface in some areas. Water depths of 3500 to 4000 m exist both north and south of the rise, which appears to be a broader feature than the Lomonosov ridge and apparently runs across the Arctic Basin sub-parallel to it. (The Lomonosov, discovered from Soviet drifting stations in 1948, extends from the New Siberian Islands across the North Pole to Ellesmere Island, dividing the Arctic Basin approximately in two.) The new rise is higher and more rugged than had at first been realized.

Bottom Materials

Submarine Photography: A Ewing suspended, automatic, submarine camera was used to take pictures of the ocean floor, the first known use of such a camera in the Arctic Ocean. Three camera stations were occupied and about 200 photographs taken in all, each picture covering about one square meter of the bottom. The stations were at 83°49′N, 165°05′W, in 2997 m of water, 83°34′N, 162°15′W, in 2300 m, and 83°49′N, 140°04′W, in 2119 m. A distance of more than 100 mi separates the first and last stations. The photographs revealed smaller features of the Arctic Ocean floor not detected by echo soundings.

An abundance of rocks of all shapes and sizes scattered about the ocean bottom is the most outstanding feature of each of these photographs. The rocks appear to be a general characteristic of the Arctic Ocean floor; such large numbers of them are not seen in bottom photographs taken in temperate latitudes. Although gravel has been dredged from the bottom by workers on IGY Drifting Station Bravo (located several hundred miles south of the last position of Station Alpha), and on Soviet drifting stations, these photographs represent the first observation of the rocks in their original positions, showing their distribution and relative situation in the sediment.

Description of Bottom Gravel: Large numbers of the rocks were brought to the surface in six dredge hauls. They are unsorted (as to size), generally subangular to angular in shape, and of many compositional types. The largest dredged was a 16-lb piece of amphibolite (a crystalline metamorphic rock composed primarily of minerals in the amphibole and plagioclase groups), but the majority of the specimens were limestone. By weight, the limestone fraction of this coarse bottom material was consistently between 50% and 70% (see

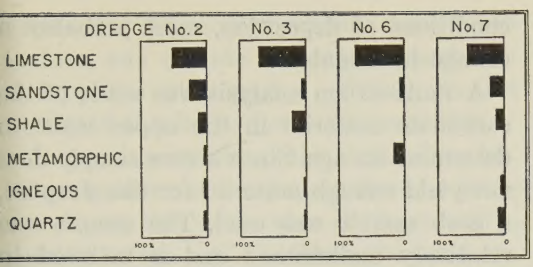

Fig. 3. *Distribution of Rock Types in Four Dredge Hauls From Drifting Station Alpha. The material analyzed was of grain size greater than 7 mm. The dredge hauls were made at the following locations: No. 2, 83° 59'N, 151° 44'W; No. 3, 84° 09'N, 150° 23'W; No. 6, 84° 28'N, 148° 28'W; and No. 7, 84° 33'N, 146° 24'W.*

Fig. 3). Straie (minute grooves scratched into the surfaces of rocks, usually by debris carried locked in glacial ice) were seen on several of the rocks. These straie, plus the lack of sorting, angularity, and heterogeneous composition of the material, point to ice-rafting as the method of deposition.

Nearly all of the larger rocks have a thin, dark manganese coating on the part that was exposed to the water, the upper part, as they rested on the bottom. Usually, more than half of the rock is covered by manganese, a sharp line separating the coated and uncoated portions showing exactly how the rock rested in the bottom sediment. Empty worm tubes, themselves coated with manganese, were found on the manganese-coated side of many of the rocks. The coating in the tubes suggests that the tubes have been empty for some time. The fact that the worms do not now thrive may be evidence of a change in bottom conditions, possibly a temperature change in the bottom waters.

Fossils of bryozoa (invertebrate colonial animals which secrete calcareous coverings) found in one of the limestone rocks identify the rock as Paleozoic in age (510–180 million years). This suggests a source area in rock layers of the Carboniferous (the coal-forming periods of the Paleozoic Era, ranging from about 255 to 205 million years ago) of the Canadian Arctic islands, or in the Devonian (315–255 million years ago) of northern Greenland. Further petrographic studies are planned to link the rocks with greater certainty to their source areas. Accurate determination of the onshore origins of these rocks will furnish clues to the drift of the ice pack in the past.

At the present time, no large detritus, or loose rock debris, is found in sea ice far from land; none was ever seen in the vicinity of Station Alpha. Thus, the pack ice in the vicinity of the station's drift path has probably never been close to shore. Only the ice islands carry large amounts of gravel at present. Hence, the rocks found on the Arctic Ocean bottom have either been dropped by ice islands or were rafted out from shore by sea ice in the past, when the ice may have drifted faster and more freely than at present.

The rocks found on T-3 (Fletcher's Ice Island), the ice island on which station Bravo is situated, are mostly metamorphics —schists and gneisses; hence, it is unlikely that T-3 is the agent which transported and dropped the sedimentary limestones and sandstones dredged from the bottom by personnel on station Alpha.

Marine Life: In several of the bottom photographs, signs of life can be seen. Tall white stalks are probably bryozoan colonies and low, rounded forms appear to be holothurians (free-living animals with elongated, more-or-less cylindrical bodies, also called "sea cucumbers") or gastropods (snails, slugs, etc.). Dredge hauls have brought up both living holothurians and living "brittle stars."

Mounds and holes, some of which may have biological origins, are present in many of the bottom photographs. It seems likely, however, that most of the mounds are buried rocks and most of the holes are impressions left by recently deposited rocks. Generally, signs of life in bottom photographs of the Arctic Ocean are sparser than in similar pictures taken in the Atlantic.

Bottom Sediment Layers: A small piston corer was used to take 15 vertical columns of sediment from the ocean bottom along the station's track. Correlations between the sediment layers are especially good for the upper parts of the cores, which average about 5 ft in length with an overall range of 1–7 ft. Previously, cores were taken in the Arctic Ocean by A. P. Crary (until recently Station Scientific Leader at IGY Little America Station and Deputy Chief Scientist, USNC-IGY Antarctic Program) and by workers on Soviet drifting stations, but the Station Alpha cores are the longest reported and hence go farthest back in geologic time.

Nearly all of the cores contain a characteristic layer, consisting of dark, foraminiferal lutite with some pebbles, extending 10–15 cm down from the top. (Foraminifera are microscopic, hard-shelled animals; lutite refers to rock composed of silt and/or clay and the various associated mud-forming minerals.) Below this layer lies a thicker layer of light-colored lutite, also containing some pebbles but relatively barren of foraminifera. The line between the two layers indicates a change in the conditions of deposition, most probably change in climate.

A radiocarbon analysis was made of th carbonate material in the upper layer t determine its age. Since a core sample doe not yield enough material for this purpos a grab sample was used. The sample wa relatively undisturbed and is believed t represent nearly the entire thickness of th top layer. The foraminifera, whose presenc would have caused errors in the datin were separated out by sieving. This wa possible because the minute animals ar nearly uniform in size.

The radiocarbon analysis, performed i the geochemistry laboratory of the Lamon Geological Observatory, yielded an age o 9300 ± 180 years. This age is post-glacia and probably represents an average for a of the post-glacial sediment in the Arcti Ocean, although the sampling method doe not allow a positive conclusion. (The Gla cial Period, or "Ice Age," is thought b many geologists to have ended about 11 000 years ago.) Some detrital material, i the form of ancient limestone fragment may have increased the apparent age by a few hundred years.

Wind Transport of Antarctic Snow

This report is based on a paper presented by William W. Vickers, Arctic Institute of North America, at the IGY Symposium during the 125th Meeting of the American Association for the Advancement of Science, Washington, D. C., December 29–30, 1958.

Two major glaciological problems are (1) determining the amount of the world's water locked up in the immense Antarctic icecap, and (2) determining whether this amount is increasing or decreasing. Closely related to the latter are investigations of the transport of snow by wind.

Wind profile studies were made on the Victoria Plateau to ascertain whether the methods of R. A. Bagnold, who correlated wind speed and the quantity of sand car ried by wind, can be adapted to studies o wind transport of snow. This report de scribes some results of these studies and o observations of the formation and move ment of sastrugi (irregular features o the snow surface formed by wind action) The work was done by William W. Vicker under an IGY contract administered by th Arctic Institute of North America.

Wind Transport

Mass-Transport Computation Method Before investigating desert sands directly R. A. Bagnold experimented with a labora tory wind tunnel. He was able to determin mathematical relationships between (1) th

wind-velocity gradient perpendicular to the surface, and (2) the quantity of sand carried by the wind past a given point. He expressed this in the form of an equation.

Bagnold pointed up the distinction between laminar and turbulent flow. In laminar flow, the molecules drift steadily, parallel to the surface. When the wind exceeds a critical value, called the Reynolds number (determined by velocity, kinematic viscosity, and, in this case, surface irregularity), turbulence sets in. In turbulent flow, the shearing, or drag, force is transmitted to the surface by the momentum of eddies, rather than by individual molecules. Instead of varying directly with the velocity, the shearing force varies with the square of the velocity. The distribution of velocity with height also differs, no longer varying with height, as in laminar flow, but with the logarithm of the height. The logarithmic profile defines the state of the wind.

Bagnold went on to show that sand movement profoundly alters the state of the wind. The wind strength at which sand of standard diameter, .25 mm, began to move by static fluid pressure alone he called the static threshold. As the load of sand being carried increased, the velocity gradient decreased, owing to the "entanglement" of the grains. This reduced velocity he termed the impact threshold. Once the grains are put into motion, a lower velocity can retain the motion by aid of the saltation principle, which states that once in flight, a grain has a potential energy which is imparted by impact to other loose-lying grains when the first grain lands, supplying the vertical component of movement for the next grain's trajectory; wind friction supplies the horizontal force (see Fig. 4).

The drop in wind momentum from static to impact threshold reflects the energy transferred to the sand grains. A quantitative analysis of this change in velocity gradient enabled Bagnold to calculate the quantity of sand being carried.

Bagnold also arrived at a slightly modified version of the wind-transport equation based on gradient. The wind velocity, v, at a given height was used instead, as follows:

$$q = \alpha C \sqrt{\frac{d}{D}} \frac{p}{g} (v - V_t)^3$$

where

α = a constant whose value varies with the surface roughness
q = quantity of sand in gm/cm width/hr
C = a constant representing the degree of natural sorting of the grain sizes (equals 1.8 for most dune material)
d = the average grain size diameter, mm
D = a standard .25-mm grain size
ρ = density of the fluid (air)
g = gravity
V_t = static threshold in cm/ sec

This equation was found best suited for the Antarctic work. (Bagnold notes the minor variation caused by density differences, such as that of snow versus sand. He shows that, compared with the much greater error caused by grain-size variation, the density difference is inconsequential.)

Comparison of Some Antarctic Profiles: Using Bagnold's method of calculation, some Antarctic wind profiles are compared in Table 1. G. H. Liljequist, on the basis of data gathered during the Norwegian-British-Swedish Antarctic Expedition of 1949–52, presented a set of profiles from which a profile can be extracted giving a wind velocity of 950 cm/sec at a one-meter height. This profile was chosen for comparison because it was found to include conditions most similar to the prevailing wind conditions on the Victoria Plateau for which transport figures are computed. A comparable profile by Bagnold is also shown in Table 1. Still another profile is indirectly available from F. Loewe, based on snow transport figures cited in his "Contributions to the Glaciology of the Antarctic," *Journal of Glaciology,* March, 1956.

The equation above has been used for all profiles in Table 1. All factors vary with the individual profile except C, D and g. All velocity measurements are at a height of one meter.

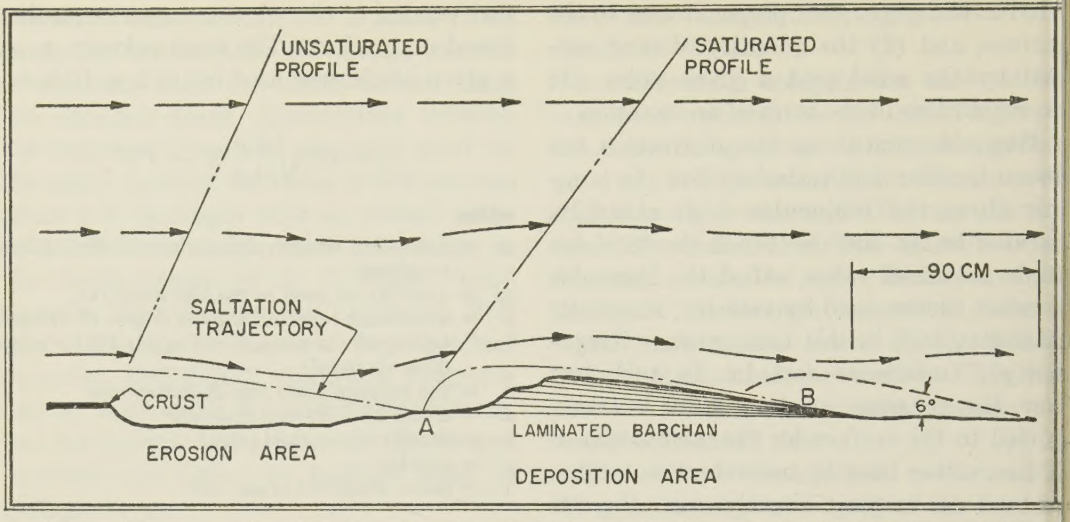

Fig. 4. *Diagram of Snow Barchan Showing the Relationship Between the Wind Profile and the Depositional Process. Comparison of the saturated and unsaturated profiles indicates the loss of velocity as the wind takes on a greater load over the erosion area.*

TABLE 1

Values of Variables and Computed Quantities of Flow

	Liljequist	Vickers	Bagnold	Loewe
k (cm)	.05	1.5	1.0	.3
d (mm)	.5	.5	.5	.5
ρ (gm/cm^3)	1.37	1.00	1.2	1.37
v (cm/sec)	950	950	950	1750
V_t (cm/sec)	270	340	400	190
q (gm/cm width/sec)	.05	.15	.12*	1.5

* A theoretical snow equivalent for sand.

The Liljequist profile is considered to be the most reliable because of high quality instrumentation and wealth of data.

Vickers' profile differs from that of Liljequist initially in the value of k, in effect, the surface roughness. (k is used in plotting the wind profile, but does not appear directly in the final formula.) This difference is thought to result from the large sastrugi on the Victoria Plateau, where surface irregularities one meter in height are common. The roughness of the Plateau surface alters the drag profile considerably; hence, the large k and V_t. The profile measurements represent an average for the apparent prevailing wind on the Plateau. The calculated snow-transport quantity shows closer correlation to Bagnold's tha to Liljequist's.

Bagnold's profile represents a prove case; a .5 mm-grain size has been substi tuted for Bagnold's .25 mm for the sake c uniformity, however, and sand density ha been converted to that of snow.

Construction of the Loewe profile re quired many dubious assumptions, whic if correct, result in fairly good correlatio for Loewe's case. However, for the sam basic figures, Loewe estimates a drift c 29 gm/cm/sec, based on the use of a cali brated snow catcher, in contrast to the fig ure of 1.5 gm/cm/sec obtained by th formula. It thus appears that there is con siderable disparity between the two possi ble methods, wind profile versus sno catcher, by which one might arrive at work ing figures for snow transport. Furthe attention to this problem may result i working figures to satisfy the factor c mass transport by wind in studies of th world's water budget.

Sastrugi Observations

Sastrugi, or skavler (synonymous term extracted from the Russian and Scandi navian tongues, respectively), means "long

crested waves." The term is used in Antarctica to include all snow-surface forms resulting from the scouring and filling action of wind. A region of sastrugi somewhat resembles a sand dune desert area, but the features are smaller and take on a greater variety of shapes (see Fig. 5).

The chief importance of sastrugi is its close relationship to the winds. It is anticipated that a knowledge of sastrugi patterns may furnish wind data for unoccupied polar regions. Its alignment, as shown in aerial photos, will give direction. Its manner of deposition and erosion, as well as its general morphology, may assist in the calculation of mass transport of snow by wind.

There are undoubtedly many ways in which a sastrugi surface may be initiated on a flat snow cover. Accordingly, sastrugi deposition as described herein is not necessarily the only way in which the phenomenon may occur.

In the desert, wind at a given height and capable of moving sand will attain a higher velocity over a pebble surface than over a sand surface. The higher velocity is reached because there is little entanglement of airborne grains over the pebble surface, since the wind strength is inadequate to start the pebbles saltating. If this same wind were then to encounter a sand surface, its speed would be abruptly checked by loss of energy to the sand load blasted into the air. The wind would drop part of this load a short distance downwind as its velocity fell and carrying power was lost, thus contributing to the growth of a dune as in Fig. 4.

On the icecap, the role of the pebble surface may be taken by any one of many types of surface crusts formed by radiation, condensation, precipitation, or sublimation. Most common, even at very high elevations, is a 2-mm crust of either milky or clear ice. The crusts offer a cemented surface as opposed to a loose-grained surface. The type of surface, of course, determines how saturated a rising wind may become; i.e., how much loose surface material is available for entrainment. The degree of grain saturation of a wind governs its capacity to scour or fill, thus dictating whether the surface forms become erosional or depositional.

The following succession of phenomena

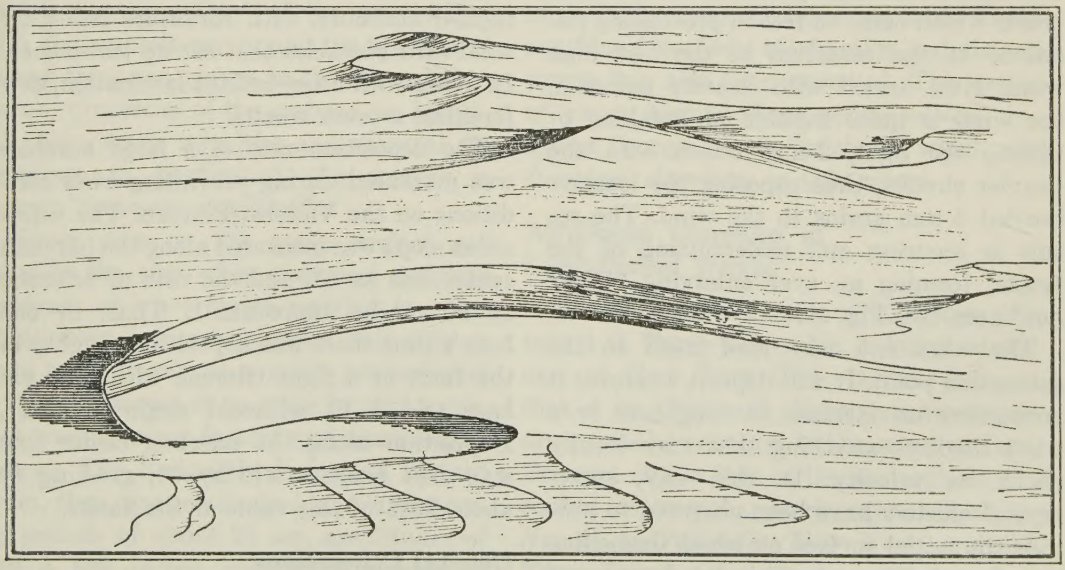

Fig. 5. *Example of Sastrugi Surface Near IGY Little America Station. The form in the foreground has been considerably eroded and sculptured by the wind. Based on a US-IGY photograph taken by Herfried Hoinkes.*

was observed to produce a loose-grained surface capable of locally retarding a drag profile, thereby causing deposition from the wind-borne load: a light precipitation of stellar and dendritic (branching) snow crystals fell under calm conditions on a smooth, cemented crust 2 mm thick. Then, a light wind rolled these crystals into clusters of about 2-cm diameter by interlocking the spikes of their branches. Further increase of wind speed swept the clusters into groups. The clusters now provided a surface of greater roughness than the smooth crustal surface. With still more wind, such clusters provide a deposition "triggering" surface.

With a large percentage of surface material originally held tightly by crusts, the wind will exceed its threshold velocity before picking up much load and being somewhat reduced in velocity by the added friction. Therefore, the wind reaches a strength capable of moving much more than the normal, loose-lying, 5-mm snow grains. Moreover, these grains, being protected by the crust, cannot be blasted into the air, to check the wind speed by their friction. However, the high velocity wind, unchecked, dislodges much larger pieces of older, broken crusts which came to rest in protruding positions at the cessation of the last high wind. Now armed with heavier material, the wind is quite capable of breaking or pitting the light, 2-mm crusts with the heavier chunks, thus exposing the loosely-bonded 5-mm grains to the wind. The result is scouring and undercutting of the crusts, forming an ever enlarging "blow-out" area (see Fig. 4).

The wind can now load itself to the saturation point. It will deposit wherever it encounters an increase in roughness or a wind shadow—anything that may locally check its velocity. In this way, snow-crystal clusters have been observed to provide the initial surface on which deposition has started. Where small isolated groups of clusters have collected, long, narrow, tapering forms are deposited in their lee, growing to several times the original cluster height. Adjacent forms often merge, eventually producing a mesa-like structure.

Snow barchans (crescent-shaped dunes), smaller than and lacking the steep "avalanche face" of sand barchans, are quite common. These are deposition forms usually found approximately one saltation trajectory downwind from an active blow-out area. The blow-out area advances downwind with the dune so that deposition-area grains are eventually in the blow-out area, and are, consequently, eroded and transported another trajectory length downwind and again deposited (Fig. 4). The dunes are quite mobile during this cycling.

Slackening of wind will elongate the dune, and a period of immobility will solidify it into a laminated "wind slab." The solidification, as explained by G. Seligman, is brought about by consolidation through the mechanical jiggling caused by saltating-grain impacts on the deposition surface and cementing of grain corners by sublimation. The lamination is due to wind sorting of grains. A very strong wind is needed to erode this now-solid slab, and migration is slow. The dunes take on spectacular contours, with curvature reflecting windward obstacles that set up turbulence. In dunes with cross-bedded lamination, differential erosion results.

The deposition rate of a large barchan was measured during prevailing-wind conditions on the Victoria Plateau. The deposition slope was measured along the barchan center line as 6°, and the rate of advance as 90 cm/hr (maximum). Thus, in one hour's time there was deposition roughly in the form of a right triangle with a 90 cm base and a 6° adjacent angle (Fig. 4). Deposition along the barchan center line was .044 gm/cm width/sec, grading to about 20% of this value at the flanks.

General Conclusions

Qualitative investigation shows the phenomenon of blowing snow in Antarctica to

be remarkably similar to that of blowing sand. Quantitative values primarily based on an established system of investigation are feasible. A correlation of these values with the wealth of wind data accumulated during the IGY would be of very great value in computing the wind-depletion factor for the Antarctic glacier mass budget.

Some Results of the IGY Island Observatory Program in the Atlantic

This report is based on material supplied by William L. Donn and William T. McGuinness of Lamont Geological Observatory, Columbia University.

The IGY Island Observatories in the Atlantic Ocean region, maintained by the Lamont Geological Observatory as part of the IGY Oceanography Program (see *Bulletins 2, 6,* and *9*), have yielded a relatively large amount of oceanographic and atmospheric data. Although much of this data will require years for complete analysis, a number of preliminary results of observations of air-ocean coupling, wave types, storm surges and sea-level changes are summarized here.

Ocean waves result primarily from wind action—the "coupling" of the sea surface with atmospheric waves and the transfer of energy from one system to the other. When certain properties of the systems are identical (here, wave velocities and physical dimensions, in particular) the process is termed "resonant coupling."

Waves seen on the ocean surface are actually the sum of a wide and complex spectrum of wave trains varying in wave length from inches to about a half mile. A wave train travels at a speed proportional to the square root of its wave length; hence, long waves travel fastest and short waves slowest. The first arrivals from a distant storm, then, are relatively long waves having periods of about 20 sec, amplitudes of only a few inches, and wave lengths of several hundred yards; often, these long, low waves can be detected only as "ground swell" where they are slowed and steepened as they traverse shallow bottoms. This ground swell is followed by a shorter, higher swell carrying most of the wave energy generated by the storm. (The word "swell" usually refers to wind-generated waves that have advanced into a region of calm or of weaker winds.) Finally, there is a shorter, lower swell as the storm effects dissipate. Alternations of high and low wave groups, often observed in the swell from a distant storm, appear to result from wave trains of different wave lengths getting in and out of step. Fluctuation in wave amplitude produced by the mixing of different wave trains is called "beating."

A wide range of oscillations intermediate in period between the tides and those waves resulting from local wind action and distant storms has also been observed. This group of waves, termed "long-period waves," includes "surges" and "seiches," which are discussed elsewhere in this report.

Air-Ocean Coupling of Long-Period Waves

Primarily on the basis of IGY data obtained at Texas Tower No. 4, 85 mi southeast of New York City, it was deduced that 4 to 12-minute dispersive air waves are coupled resonantly to the ocean surface. Pressure oscillations in the atmosphere, recorded on microbarovariographs (*Bulletin No. 9*) at Palisades, New York, and the Texas Tower, appear to travel eastward at about 40 knots along a cold frontal surface extending continuously from the eastern

coast of the United States to a distance beyond Bermuda. (A cold front is the boundary between an advancing cold air mass and a mass of warm air, under which the cold air forces its way, like a wedge.)

Velocities of about 37 knots in the air wave motion were computed from the observed ocean waves; they indicate that resonant transfer of energy is possible over a relatively broad area between the coast and Texas Tower No. 4. Such coupling is necessary to explain long-period ocean waves with heights 70 times greater than those of equilibrium barometric waves (waves whose heights just balance changes in air pressure). Since the internal air waves (those traveling within a medium rather than on its free surface) may be produced by the jet stream or other high winds aloft, the occurrence described above may represent the direct energy coupling between high-altitude winds and the sea surface.

Atmospheric Oscillations

A broad range of atmospheric pressure oscillations, from a few seconds to about 12 hours, has been recorded on microbarovariographs at all of the stations. Oscillations of 1–10 sec are clearly produced by both thermal and wind turbulence. A very striking group of constant-amplitude, constant-frequency oscillations have now been detected at many middle- to high-latitude stations throughout the world. Although these oscillations vary with time and place over the rather small interval of about 20–120 sec, a given series, which may persist for intervals ranging from a few hours to a few days, usually shows a seemingly machine-produced constancy in period and amplitude. Their detection by different types of instruments at widely separated localities in both hemispheres proves their natural origin, however. This effect has been observed only during cold weather, usually with a strong, shallow inversion aloft. Investigation is under way to determine if these constant atmospheric oscillations represent pressure variations resulting from vertical oscillations in a very stable, low-lying layer.

Another prominent group of atmospheric oscillations, with periods between about 4 and 20 min, appears to be best explained at present as surface pressure perturbations produced through the passage of internal waves along a frontal surface aloft. These oscillations often show the strong dispersion effects characteristic of wave-group propagation in a dispersive medium.

Oscillations with a semidiurnal period are usually detectable when the instruments are adjusted with appropriate time constants. These phenomena, gross compared with the micro-oscillations described above, are probably tidal (solar or lunar) in origin. For the most part, these oscillations go undetected by conventional microbarographs, or, if detected, are not resolved in adequate detail for useful analysis.

Long-Period Coastal Waves

Long-period waves seem to characterize many coastal areas, including those of relatively small islands. On the exposed southeast coast of Bermuda, these waves show characteristic oscillations of 6 to 8 min. On the southern coast of Terceira (Azores) they frequently show 8- to 10-min oscillations, while on the southern coast of Iceland, quite regular 16-min oscillations were observed during quiet-sea conditions.

These waves, which may reach amplitudes of about two centimeters, are often remarkably uniform (sinusoidal) in shape; in addition, they seem to have a spectrum unique to a particular area. These waves have been recorded on underwater pressure heads, instruments sensitive to changes in pressure produced by wave motion and usually installed at a depth of 30 ft. Most of the instruments are located off open coasts or coasts having a broad concave curvature; hence, the oscillations are not likely to be a function of harbor resonance.

During local storms, a complex spectrum

of long-period oscillations with periods ranging between about 1 and 25 min was found to exist in coastal regions. Such oscillations have not yet been detected at Texas Tower No. 4, which stands in about 30 fathoms of open water. This, together with the characteristic period relationships, suggests that the oscillations are a coastal resonance phenomenon rather than a simple coastal amplification of long waves traveling in from the ocean.

Coastal and Deep-Water Waves

Comparison of both short- and long-period wave recordings from the Texas Tower with those from coastal installations, both island and continental, shows a rather striking contrast. All wave records made in the relatively open ocean area in which the tower stands appear in striking sinusoidal groups, suggesting a relatively narrow power range. Short-period (gravity) waves recorded in deep water occur in very uniform, undistorted groups, closely resembling classical beat patterns. Waves recorded in shallow water off coasts show far more irregular patterns, indicating a greater spread of frequencies, more complex interference from coastal reflections, or a combination of both.

Long waves recorded in deep water also appear smoother than those offshore. As noted above, the characteristic low-frequency waves have not been recorded, and it appears thus far that most such waves in deep water are related to similar oscillations in the atmosphere. Another very striking difference between coastal and deep water long-wave records is the strong "surf beat" indicated by the former, particularly at times of strong short-wave activity, and the complete absence of surf beat in the deep-water records. (Surf beat refers to irregular oscillations of the near-shore water level at intervals of several minutes.) These observations support the explanation of surf beat as a coastal effect resulting from the mass transport of water through wave-group activity. A maximum amplitude of several inches was observed when such activity was high.

Storm Surges in the Lesser Antilles

Islands of the Lesser Antilles, particularly Barbados, the easternmost, have long been beset by severe and damaging sea surges. (Surges have periods generally between about 30 sec and 1 hr and are usually less than .3 ft high.) These sea surges, which may continue for a day or more, arise with little warning and are unrelated to local weather. Attempts to explain them in terms of submarine landslides or earthquakes have proved unsuccessful. Four occurrences of sea surges have now been explained, however, by means of IGY data.

Intense North Atlantic storms having the appropriate fetch (distance the wind blows over the water in a particular direction) can generate long-period ocean swell (15–20 sec) spreading toward the Lesser Antilles. If the swell maximum arrives at low tide, much of its energy is expended on the outer reefs. If it arrives at high tide—particularly spring high tide—the long-period swell crosses the reef and develops high and damaging surf at the shore. If the swell maximum is protracted, surf conditions vary with the tide until the swell subsides.

From these studies, it now seems possible to forecast sea surges two or more days ahead through storm locations shown on synoptic charts and allowance of appropriate travel time for the swell generated.

Seiche Observations

Because the tide gauges were installed on long piers usually located in sheltered water bodies, seiche oscillations of these water bodies have been well recorded. (A seiche is an oscillation whose period, generally from a few minutes to an hour or more, is determined by the basin's physical dimensions.) Most seiches are of meteorologic origin, but possible coupling to seismic surface waves is being investigated. Simple

periodicities were recorded only by instruments located in uniformly enclosed harbor or bay regions. Elsewhere, the seiche spectrum may be continuous, as at Grindavik, Iceland, or discontinuous, as in St. George's Harbor, Bermuda.

Grindavik exhibits a 12-ft tide range; superimposed on the tide wave is a seiche with a period spectrum of 4-10 min, varying directly with sea-level height. At high tide, the size of the oscillating area increases from flooding and the average depth of the oscillating basin decreases, giving the observed effect. At Bermuda, seiche oscillations show fairly discrete periods of 10 and 40 min. The shorter period is associated with the smaller water body at St. George's Harbor, and the longer with the much larger water body shoreward from the outer reef of the Bermuda platform.

Sea-Level Changes

Certain sea-level phenomena must be related to temporary current changes and probably reflect a local variation in the vertical ocean structure. An example of local variation is the anomalous drop in sea level of 0.75 ft recorded in August 1958 at Bermuda (supported by independent observations of the US Coast and Geodetic Survey). In September, sea level returned to its July value.

Fifth US-IGY Earth Satellite

The fifth US-IGY satellite, 1959 Alpha (Vanguard II), was launched from Cape Canaveral, Florida, at 10:55 am EST on February 17, 1959. It was injected into orbit 10 min later. The launching vehicle, the three-stage, 72-ft, 22,600-lb Vanguard rocket developed by the US Naval Research Laboratory, was essentially the same as that used to put 1958 Beta (the Vanguard I test sphere) into orbit (see *Bulletin No. 11*).

The cloud-cover satellite, a project of the National Aeronautics and Space Administration (NASA), was instrumented to measure cloud-cover distribution over the daylight portion of its orbit. These data will be related to the over-all meteorology of the earth.

Satellite Characteristics: 1958 Beta is a sphere 20 inches in diameter and weighing 21.5 lbs. The outside is plated with pure gold polished to a mirror-bright finish. This highly reflective surface was designed to balance radiation from the satellite against the heat from the sun and from the satellite's batteries, providing a sufficiently cool environment for proper functioning of the instrumentation. The 5.5 × 12-in, cylindrical instrument package is supported by an internal framework of magnesium tubing. (See Fig. 6).

Cloud-Cover Experiment and Instrumentation: The cloud-cover experiment developed by the US Army Signal Research and Development Laboratory at Fort Monmouth, N. J., utilized two photocells, each at the focus of one of two optical telescopes aimed in diametrically opposite directions at an angle of 45° from the spin axis of the satellite. As the satellite circled the earth, the photocells measured the varying intensities of sunlight reflected from clouds (about 80%), land masses (15–20%), and sea areas (5%). The satellite's spin, about 50 rpm, caused the photocells to scan the earth in successive lines, producing a lined picture not unlike a television picture.

The measured reflection intensities were converted into electrical signals, which were stored in a tape recorder within the instrument package. Separate solar batteries turned on the recorder only when the

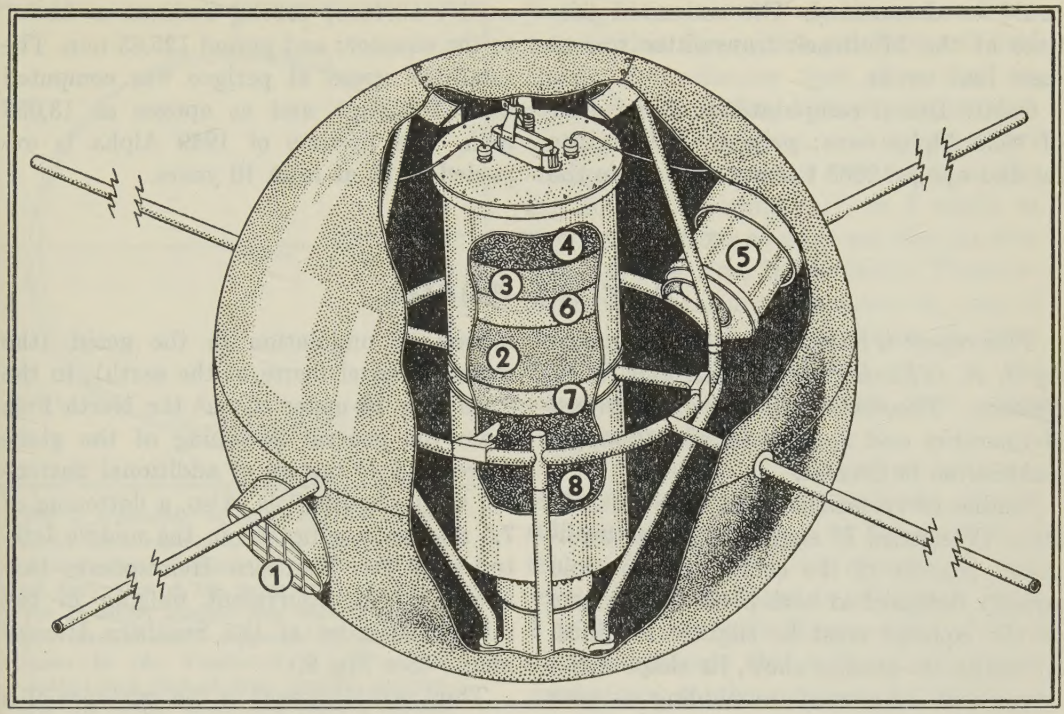

Fig. 6. *Cutaway Diagram of Satellite 1959 Alpha. The instrumentation consists of (1) photocell light shields, (2) recorder, (3) interrogation radio receiver, (4) meteorological data transmitter, (5) photocell, (6) data electronic equipment, (7) tracking transmitter, and (8) mercury-cell batteries. From US Army photograph.*

earth beneath the satellite was in daylight, giving 50 min of data per orbit. The 75-ft loop of recording tape accommodated all scanning data from the sunlit part of a single orbit. Once in each orbit, a selected ground station interrogated the satellite by signalling a command receiver within the satellite, causing the entire tape to be played back in 60 sec. The tape was then "erased" and the system triggered to begin recording again. At the interrogating ground station, the data were received on a wide-band magnetic tape recorder and the tape was immediately air-mailed to the US Army Signal Research and Development Laboratory for analysis and conversion into cloud-cover pictures.

The experiment was designed to obtain cloud-cover data between the equator and 35° to 40° north latitude. (Although the satellite's orbit covered an equivalent area south of the equator, most of this region was in darkness during the times the satellite passed over it.) According to the original plan, cloud-cover data was to be obtained for 600-mile-wide strips on each pass, totaling about 25% of the earth's sunlit surface in a 24-hour period. The exact coverage, however, depends upon the many orbital variables.

Radio Equipment: The radio transmitter for the cloud-cover experiment used a frequency of 108.03 megacycles at a power level of one watt, modulated by signals from 2500 to 12,500 cycles/sec. The expected lifetime of the batteries for both the experiment and its radio transmitter was at least two weeks. The Minitrack transmitter sent a continuous, unmodulated signal at 108.00 mc with a power level of 10 milliwatts. This transmitter carried a temperature-sensitive quartz crystal which varied the frequency such that the internal temperature of the instrument package

could be determined. The estimated lifetime of the Minitrack transmitter was at least four weeks.

Orbit: Initial computations of the orbit of 1959 Alpha were: perigee 346.9 statute mi and apogee 2065.1 statute mi above the earth's surface; orbital inclination 32.86° to the equator; and period 125.85 min. The satellite's speed at perigee was computed as 18,312 mph and at apogee as 13,093 mph. The lifetime of 1959 Alpha is expected to be at least 10 years.

Earth's Shape

This report is based on material prepared by J. A. O'Keefe, Ann Eckels, and R. K. Squires, Theoretical Division, National Aeronautics and Space Administration, for publication in Science.

Studies of variations in the orbit of 1958 Beta (Vanguard I) suggest that the traditional concept of the earth as a spheroid equally flattened at both poles and bulging at the equator must be slightly modified. Actually, the studies show, its shape has a component somewhat resembling a pear (see Fig. 7).

Certain variations in satellite orbits are attributable to regional differences in the earth's mass, or, more specifically, differences in the gravitational force acting on the satellite. Since such orbital variations are periodic, the gravitational variations which cause them can be analyzed in terms of harmonic components. There are many types of harmonics, which, when plotted graphically, appear as waves; those which vary with latitude only are termed "zonal harmonics."

Calculations show that periodic variations in the orbit of 1958 Beta can be explained by a third zonal harmonic in the earth's gravitational field. The third zonal harmonic appears as three waves, each equal to one-third the circumference of the earth. The amplitude of this third zonal harmonic—that is, the extent to which its maximum gravity values vary from the average—is 4.7 milligals. (A milligal, or mgal, is one-thousandth of a gal, which is an acceleration due to gravity of one cm/sec^2.) This gravity variation implies 15 meters of undulation in the geoid (the mean-sea-level figure of the earth), in the form of a 15-meter rise at the North Pole from the general flattening of the globe there, and 15-meters of additional flattening at the South Pole. Also, a flattening of 7.5 meters is indicated in the middle latitudes of the Northern Hemisphere, balanced by an equivalent bulging in the middle latitudes of the Southern Hemisphere. (See Fig. 8.)

Thus, establishment of the existence of a third zonal harmonic requires slight modification of the geoid toward the shape of a pear, with the stem end up, i.e., at the North Pole.

In principle, the perturbation of the 1958 Beta orbit might be caused by harmonics with either an odd or an even number of waves. The even harmonics can be excluded as a cause, however, because they would show similar effects in both hemispheres, whereas the actual observed effects are opposite in the Northern and Southern Hemisphere. Harmonics which depend on longitude as well as latitude (known as tesseral harmonics) can also be excluded, because these too are the same in both hemispheres, apart from a shift with longitude. This leaves only the zonal harmonics of odd degree as possible explanations of the variations in the orbit of 1958 Beta.

Of these odd harmonics, the first degree is nearly zero because the center of the system on which the computations are based —the Vanguard coordinate system, set up by the Army Map Service—coincides with the earth's center, to an accuracy of about

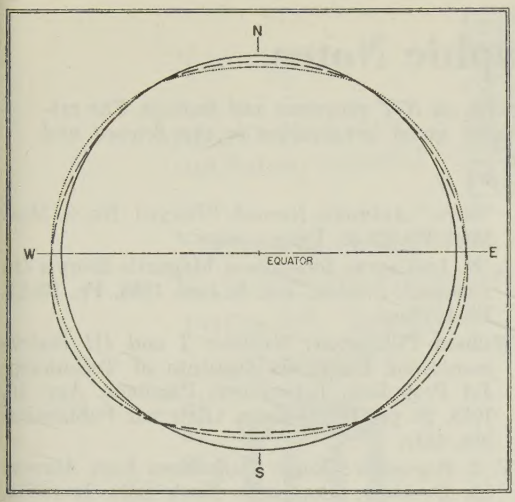

Fig. 7. *Concepts of the Earth's Shape. Solid line represents a perfect sphere; dotted line indicates the traditional view of flattening at the poles and bulging at the equator; dashed line depicts slightly pear-shaped earth suggested by perturbations in the Vanguard I orbit. Both dotted and dashed lines greatly exaggerate the actual deviations from a perfect sphere. The exaggeration of the dashed lines is especially great in order to emphasize the new findings; actual distances at the poles from the solid to the dotted line are about 1000 times as great as from the dotted to the dashed line.*

100 m. Accordingly, the first zonal harmonic is much too small to produce the observed effect. Odd harmonics of high degree are unlikely to have a large effect because they die out inversely as the $(n + 1)$ power of the distance from the earth's center, where n is the degree of the harmonic.

By a process of elimination, therefore, it was concluded that the perturbation in the satellite orbit is due mostly to the third zonal harmonic, with a possible contribution from the fifth.

By applying to the variations observed in the orbital elements of 1958 Beta certain relations derived by H. Jeffreys, the value of 4.7 ± 0.4 mgal for the third zonal harmonic of gravity at the earth's surface is obtained. This finding contrasts with the "basic hypothesis of goedesy" of F. A. Vening Meinesz and W. A. Heiskanen. They assume that the earth's gravitational field closely approximates that of a fluid in equilibrium and that deviations from such an ellipsoid in any given area do not exceed 30 mgals over an area of 1000 km on a side, i.e., 30 mgal(megameter)^2, or 3 mgals as gravity variations average out over an area 3000 km on a side. In the NASA Theoretical Division calculations, however, each of the polar areas has a deviation of about 120 mgal(megameter)^2 and each of the equatorial belts a deviation more than twice as great.

The presence of a third zonal harmonic of this large amplitude indicates a very substantial force acting on the surface of the earth. Following the methods of Jeffreys, this crustal load is calculated to be 2×10^7 dynes/cm^2. Hence, either stresses of approximately this order of magnitude exist down to the core of the earth, or stresses about four times as great exist in the uppermost 700 km only. These stresses must be supported either by a mechanical strength greater than usually assumed for the interior of the earth, or by large-scale convection currents in the earth's mantle.

The orbital data for Vanguard I was furnished by the Vanguard Minitrack Branch, under the direction of John T. Mengel; by the IBM Vanguard Computing Center, under the direction of Joseph W. Siry; and by Paul Herget, then consultant for the Naval Research Laboratory.

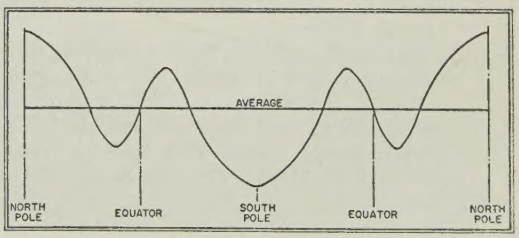

Fig. 8. *Symbolic Representation of the Third Zonal Harmonic of the Earth's Gravitational Field. (Not drawn to scale.)*

IGY Bibliographic Notes

This is the ninth of a series of bibliographic notes on IGY programs and findings. The references are selected largely from an IGY bibliography under preparation in the Science and Technology Division of the Library of Congress.

Sh. A. Bezverkhnii and P. M. Broitman: First Results of Ozonometric Observations During the IGY (in Russian). *Vestnik.* No. 8. Akademii Nauk Kazakhskoi SSR. Aug. 1958. Pp. 27–31. Diagr.

E. G. C. Burt: The Computation of Orbit Parameters from Interferometer and Doppler Data. *Proceedings of the Royal Society.* Ser. A, Vol. 248. Oct. 28, 1958. Pp. 48–55. Diagr.

Further Advances on a Broad Front. *Discovery.* Vol. 19, no. 11. Nov. 1958. Pp. 475–476. Map.

Jacques Gilbert: Premiers Résultats des Sondages Aérologiques Effectuées en Terre Adélie pour l'Année Géophysique Internationale. *Comptes Rendus des Séances de l'Académie des Sciences.* Vol. 247, no. 1. Jul. 7, 1958. Pp. 118–121.

K. I. Gringauz: Rocket Measurements of Electron Concentration in the Ionosphere by Means of an Ultra-short Wavelength Dispersion Interferometer (in Russian). *Doklady.* Vol. 120, no. 6. Akademiia Nauk SSR. 1958. Pp. 1234–1237.

Albert R. Hibbs: The Earth Satellite Program. *Astronautics.* Vol. 3, no. 11. Nov. 1958. Pp. 34, 110–116.

Kou Kusunoki: Preliminary Report on Oceanographic Observation of the Japanese Antarctic Research Expedition I, 1956–1957, with the "Soya." *Antarctic Record.* (Tokyo). No. 3. M[illegible] 1958. Pp. 32–40. Diagr., maps.

L. N. Liakhova: Ionosphere Magnetic Storms (Russian). *Priroda.* No. 6. June 1958. Pp. 89–[illegible] Illus., diagr.

William Pilkington: *Explorer I and III Instr[illegible] mentation.* California Institute of Technolo[illegible] Jet Propulsion Laboratory, Pasadena. Apr. [illegible] 1958. 24 pp. Illus., diagr. (External Publicati[illegible] No. 482).

V. I. Pogorelov: *Radar Reflections from Auro[illegible] (in Russian).* Akademiia Nauk SSR. Izvesti[illegible] Seriia Geofizicheskaia, No. 8. Aug. 1958. H[illegible] 1048–1051.

M. Ryle: Observations at the Mullard Radio A[illegible] tronomy Observatory, Cambridge. *Proceedi[illegible] of the Royal Society.* Ser. A, Vol. 248. Oct. [illegible] 1958. Pp. 3–9. Diagr.

Results of Investigations of the Institute Oceanology in the Pacific Ocean (in Russian [illegible] *Vestnik.* No. 9. Akademiia Nauk SSR. Sep[illegible] 1958. Pp. 97–98.

K. Weekes: The Ionosphere and the Radio Emi[illegible] sion from the Satellites. *Proceedings of t[illegible] Royal Society.* Ser. A, Vol. 248. Oct. 28, 19[illegible] Pp. 77–80.

Data Center Reports

Rocket and Satellite Report Series: The following numbers of the IGY World Data Center A Rocket and Satellite Report Series have been issued since the last announcement (see *Bulletin 19*). They are available from the National Academy of Sciences at $1.00 each:

Satellite Report No. 7—Simplified Satellite Prediction from Modified Orbital Elements.

Rocket Report No. 2—Flight Summaries for US Rocketry Program for the IGY, Part I: 5 July 1956–30 June 1958 (in preparation—Part II: 1 July 1958–31 December 1958).

Glaciological Report Series: Not available from the National Academy of Sciences. May be obtained at $3.00 per copy from:

IGY World Data Center A: Glaciology
American Geographical Society
Broadway at 156th Street
New York 32, New York

No. 1—Preliminary Reports of the Antarctic and Northern Hemisphere Glaciology Programs (July 1958). Second edition, without illustrations.

No. 2—Further Reports on the IGY glaciology program in Antarctica (in preparation —title tentative).

Preprinted from *Transactions, American Geophysical Union,* Vol. 40, No. 2, June 1959